Building Tomorrow's Society
Bâtir la Société de Demain

Fredericton, Canada
June 13 – June 16, 2018/ *Juin 13 – Juin 16, 2018*

TRADITIONAL VS COLUMN-TOP ISOLATION FOR TYPICAL STRUCTURES

Darlington, Richard E.[1,2] and Becker, Tracy C.[1]
[1] McMaster University, Canada
[2] Darlinr@McMaster.ca

Abstract: Traditional installations of base isolation can be expensive, especially in retrofit applications. Addition of a rigid diaphragm above the isolation layer, excavation of a seismic moat, and extensive foundation work increase construction time and costs. As a result, isolation retrofit projects are typically limited to buildings with historic significance and large budgets. Limiting the use of isolation to new and/or large budget structures means fewer buildings are likely to remain functional post-disaster, decreasing community resilience during large earthquake events. To make isolation retrofit accessible to a wider range of structures, the up-front costs must be reduced. This can be achieved by placing bearings on column tops, forgoing the need for construction of a seismic gap and an additional rigid diaphragm. However, columns under the isolation layer may be flexible, changing the traditionally assumed bearing end conditions. To assess the viability of column-top isolation, the performance of a pre-Northridge steel moment resisting frame office building, designed to the 1965 National Building Code of Canada (NBCC), is compared against a column-top retrofit with stiffened first floor columns and a traditional base isolation retrofit design using lead-core rubber bearings. This study also explores the impacts of gravity frame modelling assumptions in moment resisting frame structures on the performance of the isolated systems. Suites of ground motions representing different fault types were selected and scaled to hazard levels prescribed in the 2015 NBCC. Using a nonlinear time history analysis in OpenSEES, the overall seismic performance of column-top isolation was investigated.

1 INTRODUCTION

Many structures designed to older, less stringent building codes are at risk of significant damage or collapse in large scale earthquakes (Kunnath et al., 1995). Of particular concern are pre-Northridge steel moment resisting frames (MRF) with connections that have a high probability of fracture under moderate story drifts (Ramirez et al., 2012). While isolation is an effective method for improving both structural and nonstructural performance, retrofit using traditional base isolation in existing structures is expensive due to the costs of excavation, foundation work, and construction of a rigid diaphragm as shown in Figure 1. This cost limits the types and number of structures to which isolation may be employed. An alternative form of isolation involves placing the flexible isolation layer on top of the first floor columns, which helps mitigate many of these costs.

The ratio of the isolation layer stiffness to fixed base structure stiffness is an important parameter in isolation; however, older moment frame buildings are often quite flexible. While building stiffness is often thought of in terms of the lateral load resisting frame, the gravity frame can have a significant contribution. The connections of the beams and columns in the gravity frame are typically considered pinned and their stiffness contribution is neglected. AISC specifies a rotational stiffness under which the stiffness contribution of the connection is ignored (AISC, 2016). However, Liu and Astaneh-Asl (2000) performed cyclic tests on gravity frame shear tab connections with rotational stiffness values below the AISC threshold, showing that

bare steel shear tabs can achieve up to 20% of the beam's plastic moment capacity. Thus, a semi-rigid connection assumption may be more realistic when modeling the gravity frame, which can improve isolation performance by further separating the isolation and superstructure periods.

This study compares the performance of a typical steel moment resisting frame office building designed to the 1965 National Building Code of Canada against a column-top retrofit and a base isolation retrofit (NRCC, 1965). The building is located in Vancouver, British Columbia with soil class D. For the isolation retrofits, lead core elastomeric isolators are used. Figure 1 presents the configuration of the isolation system building for both the pre- and post-retrofit layouts. Gravity beam-column fixity and their impact on the effectiveness of isolation retrofits are explored to assess the contribution of simple shear tabs to the behavior of the column-top isolated structure. The models are subjected to a suite of 15 ground motions representing crustal, inslab, and subduction maximum considered earthquakes (MCE) selected and scaled to the hazard levels prescribed in the 2015 NBCC (Tremblay et al., 2015). Three-dimensional nonlinear time history analyses for the pre-retrofit, column-top retrofit, and base isolation retrofit frames were conducted in OpenSees (McKenna and Fenves, 2006).

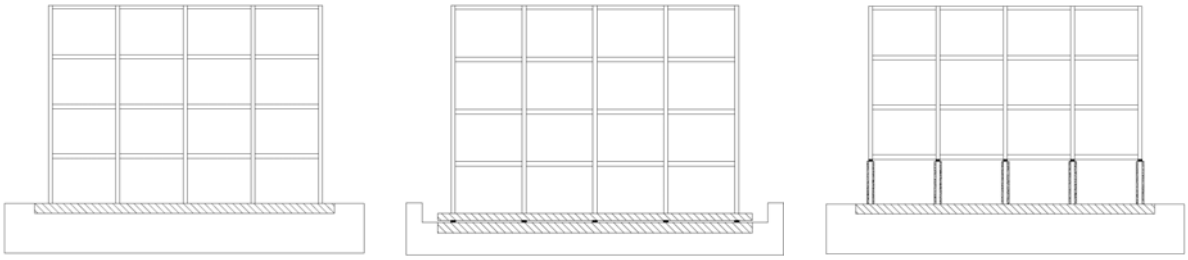

Figure 1: Structural layout of the pre-retrofit MRF, base isolated MRF, and column-top isolated MRF

2 BUILDING DESIGN

The building has two moment resisting frames in both principle directions on the perimeter of the building. The building is four floors each with 4 m height. The footprint is four bays by eight bays long with 6 m spacing between columns in both directions. The 1965 National Building Code of Canada (NRCC, 1965) was used for the pre-retrofit building design due to the large amount of building stock from this era. For earthquake loading, the code prescribed a simple method of calculating the design base shear *V* as

[1] V = K•W

where *K* is the minimum design load parameter and W is the seismic weight due to dead load plus any loads from storage, service equipment, and machinery. The minimum design load parameter was found as

[2] K = R•C•I•F•S

where *R* is the earthquake factor, C reflects the type of construction, I reflects the importance of the building, *F* reflects the site conditions, and *S* reflects the number of stories in the building. The individual factors are defined as follows:

- The earthquake factor *R* attempts to capture the amount of hazard present at a given location and was determined from a seismic zoning map. The map was developed by Hodgson (1956) using a qualitative assessment of the historical seismicity in Canada to identify four zones based on the amount of seismic risk in each zone. An earthquake factor of 4 was taken for this study.

- The construction type factor *C* is used to capture the ductility capacity of the structure. For steel or concrete moment resisting frames with rigid diaphragms and where the frame alone is able to carry 50% of the design shears, a value of 0.75 is used. For any other types of construction used, a value of 1.25 is assigned. The construction factor was taken as 0.75 for this study.

- The importance factor *I* is similar to current codes. For important structures, a value of 1.3 is used, while all other buildings have an importance factor of 1.0. The importance factor was taken as 1.0 for this study.
- The foundation factor *F* attempts to capture soft soil effects. The factor is of 1.5 for building sites with highly compressible soil and 1.0 for all other soil conditions. The foundation factor was taken as 1.0 for this study.
- The story factor *S* is used to capture structural period specific demand. The factor is calculated as

$$[3]\ S = \frac{0.25}{9+N}$$

where *N* is the total number of stories in the building. The factor reduces the shear for taller buildings. Calculated to be 0.019 for this study. These factors resulted in a minimum design load parameter of *K* = 0.058, meaning a base shear coefficient of 5.8%. Using the prescribed seismic weight, a base shear of 1196 kN was obtained. The base shear was then distributed to each floor similarly to current code equivalent static method. By comparison, assuming a ductile moment frame, the seismic load provisions in the 2015 NBCC resulted in a base shear of 7.2% kN, approximately 24% larger than the 1965 code.

The historical code prescribed no limits to the lateral deflection but specified that adequate stability must be provided. Modern interstory drift limits of 2.5% were used to ensure stability of the structure. The selected sections, summarized in Table 1, were designed based on design provisions in the CSA S16-14 steel code (CSA, 2014). All members were assumed to have A36 grade steel with a yield strength of 250 MPa, based on the availability of steel products during the time period under consideration (CISC, 2014). The interior gravity columns and beams were selected as W250x67 and W310x33 sections respectively.

Table 1: Selected moment frame sections

Element	Columns	2nd Fl Beams	3rd Fl Beams	4th Fl Beams	Roof Beams
Section	W310x158	W410x67	W410x60	W360x51	W310x33

2.1 Isolator Design

Two retrofits strategies were designed, one using a column-top isolation strategy by shortening the first story columns to accommodate lead-core rubber bearings without changing the floor heights and the other as a traditional base isolated structure. Crowder and Becker (2017) experimentally investigated hysteretic properties of natural rubber bearings placed at the top of columns of increasing flexibilities. It was found that with very flexible columns, the nonlinear behaviour of the bearing varied significantly from typical rubber bearings; however, with stiffer columns, the bearing lateral and rotational behavior can be well predicted by simplified models as the stiff end conditions resulted in minor decreases in the lateral stiffness. From this, Crowder and Becker proposed a 10% limit for the ratio between the post-yield horizontal stiffness of the bearing to the lateral stiffness of the column where the stiffness ratio is defined as

$$[4]\ SR = \frac{k_b}{k_c} = \frac{GA/t_r}{3(EI)_c/L^3}$$

Lead-core rubber bearings are used instead of natural rubber bearings as the additional hysteretic damping is necessary to limit the displacements. The isolation system was designed assuming the bearing endplates remain parallel, although it should be noted that the flexible end conditions will decrease the lateral stiffness of the bearings leading to a longer period than calculated (Crowder and Becker, 2017). In addition, the buckling load of the bearings was determined assuming fixed-free conditions following the work by Imbimbo and Kelly (1997) in order to provide a conservative estimate. The design objectives for the isolators were a period of 2.5 seconds, 10% effective damping, and a confining pressure of 2 MPa. A displacement limit of 90% of the bearing diameter was used. The light axial loads on the bearings made it difficult to achieve a long isolation period and thus, separation from the fixed base period. The relevant properties for the bearing

designs are available in Table 2. The peak bearing displacements were expected to reach 328.8 mm based on the 2% in 50 years design spectrum, 89% of the diameter of the column-top bearing or 78% of the diameter of the traditional isolation bearing.

For the column-top retrofit, there is a concern about the stiffness of the gravity and lateral load resisting system columns when bending about their weak-axis as there is no longer a diaphragm below the isolators. The first floor columns were stiffened using concrete and rebar to create composite column sections. They were designed based on the stiffness of the weak axis. The new interior and exterior first floor column dimensions were designed to be 650x650 and 620x620 respectively. The stiffness ratios for the interior and exterior columns were 4.8% and 4.5% about the weak axis, respectively.

Table 2: Bearing design values

Property	Column-Top Interior (Corner)	Base Isolated Interior (Corner)
Radius (mm)	185	210
Radius of lead (mm)	28	35
Yield of Lead (MPa)	10.3	10.3
Rubber layer thickness (mm)	5	5
Steel layer thickness (mm)	3	3
Total rubber thickness (mm)	130	105
Total height (mm)	201	165
Shape factor	15.7	17.5
Shear modulus (MPa)	0.4	0.4
Applied pressure (MPa)	5.69 (2.13)	6.99(2.19)
Buckling pressure (MPa)	15.8	23.1

2.2 Building Modeling

Nonlinear time history analyses of the original MRF, column-top retrofit frame, and base isolated frame were conducted using OpenSees (McKenna and Fenves, 2006). The buildings were modelled in three dimensions in order to capture the proper distribution of isolator and first-floor column retrofit stiffness, but only unidirectional ground motions are used. All beams and columns were modelled with displacement-based beam columns constructed with fiber sections. The stress-strain behaviour of the steel was modelled with a Giuffré-Menegotto-Pinto hysteretic model. The first-floor composite column concrete used in the column-top retrofit was represented by the Concrete02 hysteretic material, using the Mander model to describe the behaviour of the confined concrete with a 1.3 strength multiplier. Yield strength of the concrete was taken as 40 MPa and the rebar yield strength was taken as 400 MPa. Two percent stiffness proportional damping was applied only to the superstructure. The isolation bearings used in the column-top and base isolated frames were modeled using the LeadRubberX open-source bearing element (Kumar and Whittaker, 2015). This element was chosen as it includes rotational stiffness, an important consideration associated with the non-parallel end conditions that may be found in column-top isolation.

Three cases were modelled and compared for the gravity frame connections: pinned, semi-rigid, and rigid. Table 3 presents the fundamental periods for the three connection cases with the original fixed base MRF, the base isolated building, and the column-top isolated building. The semi-rigid connections were modelled using a locally weakened fiber element of the beam web (Jones et al., 1983). The plastic section modulus of the web element was 23% of the parent beam member. Liu and Astaneh-Asl (2000) conducted cyclic testing of simple shear tab connections, with and without the contributions of the floor slab and showed that bare steel simple connections can develop up to 20% of the beam plastic moment capacity. Testing with the floor slab contribution led to doubling of the peak moment capacity. As a result, it was concluded that a fiber element representation with 23% of the beam capacity was suitable for the purposes of this study. In the case of this typical office building, incorporating semi-rigid connections resulted in a significantly lower fundamental period than the pinned case, showing that incorporating gravity connection fixity in the model

can significantly impact the elastic stiffness of the superstructure. Using the pinned gravity frame modelling assumption resulted in isolated fundamental periods that are not as well spaced from the fixed base superstructure.

Table 3: First Mode Fundamental Periods

	Pinned (s)	Semi-Rigid (s)	Rigid (s)
MRF	2.12	1.65	1.49
Column-top	3.03	2.81	2.72
Base Isolated	3.07	2.82	2.73

3 NUMERICAL RESULTS

3.1 Ground Motion Selection and Scaling

The ground motions used in the analysis were selected from those identified by Goda and Atkinson (2011) and scaled to the to the uniform hazard spectra values for the 2015 NBCC for site class D in Vancouver. Scaling was done following the procedure outlined in Tremblay et al. (2015) which identified three classes of earthquakes that contributed to the seismic hazard in Vancouver as well as the period ranges over which each class has a significant contribution. Shallow crustal earthquakes were found to contribute predominantly at periods less than 0.8 s, deep inslab events were found to contribute from 0.3 to 1.5 s, and subduction earthquakes were found to contribute at periods greater than 1.0 s. Five ground motions of each class, scaled within their respective ranges, were selected for the study from the PEER-NGA and K-NET, KiK-net databases. Comparisons of the response spectra to the ground motions and their respective scale ranges can be found in Figure 2.

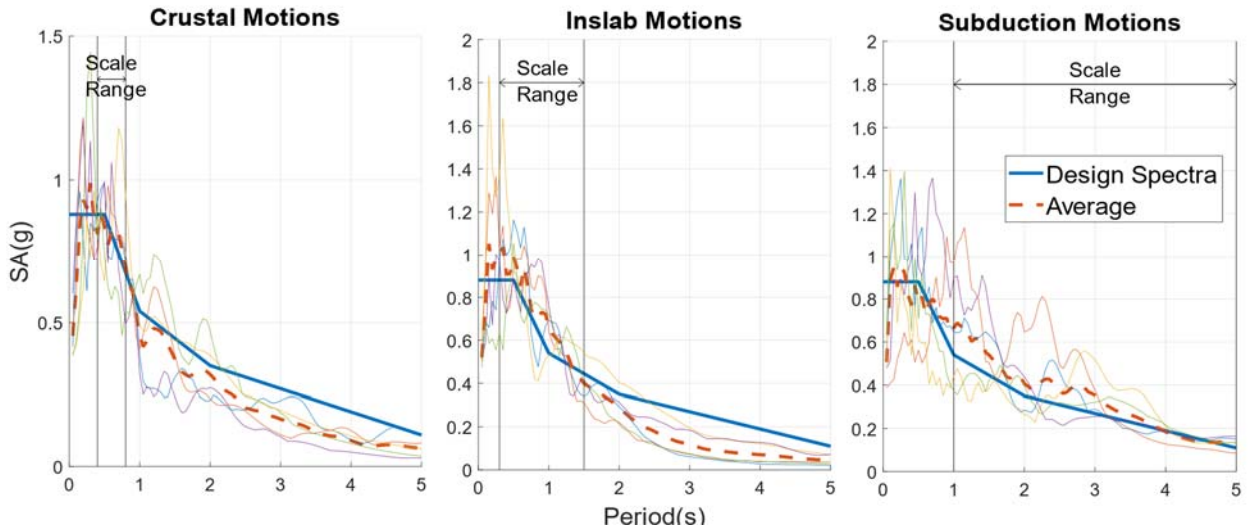

Figure 2: Ground motions, 5% damped spectra

3.2 Collapse Limits

Collapse is determined by excessive interstory drifts, excessive bearing displacements, or numerical model instability signalling from isolator stability limits. Drift limits for the pre-Northridge beam to column connections were taken from a structural component database (Lignos and Krawinkler, 2012). Table 4 provides the median story drift ratios (SDR) at which beam-column fracture occurs as a function of the length to depth (L/D) ratio of the beam (Ramirez et al., 2012). A 2.5% story drift ratio was taken as a collapse limit. The bearings were assumed to fail after they reach a displacement of 90% of their diameter or their buckling limit.

Table 4: Pre- Northridge Fracture Damage State Drift Ratio

Floor	Beam-Column L/D Ratio	d (mm)	Median Fracture SDR (%)
2	14.0	410	2.1
3	14.0	410	2.1
4	16.0	360	2.15
Roof	18.0	310	2.25

3.3 Performance Comparison

A summary of the analysis results is shown in Figure 3, highlighting the number of motions resulting in collapse, yielding, or elastic behavior. Yielding begins at roughly 1% story drift. The isolated structures provided enhanced performance in crustal and inslab ground motions; however, the long period subduction motions caused significant yielding or collapse in all of the structural systems under all fixity assumptions. The MRF structure either yielded or collapsed in all ground motions regardless of the fixity assumption made. The MRF structured collapsed of 87% of the ground motions with pinned gravity beam-column connections. This was reduced to 40% with semi-rigid gravity beam-column connections. Modelling with the semi-rigid gravity connection assumption resulted in an average reduction of interstory drift of 19%. This value is in line with previous numeric studies where average drift reductions of 22% were achieved in pushover testing by considering the contributions of gravity connections (Barber et al., 2011).

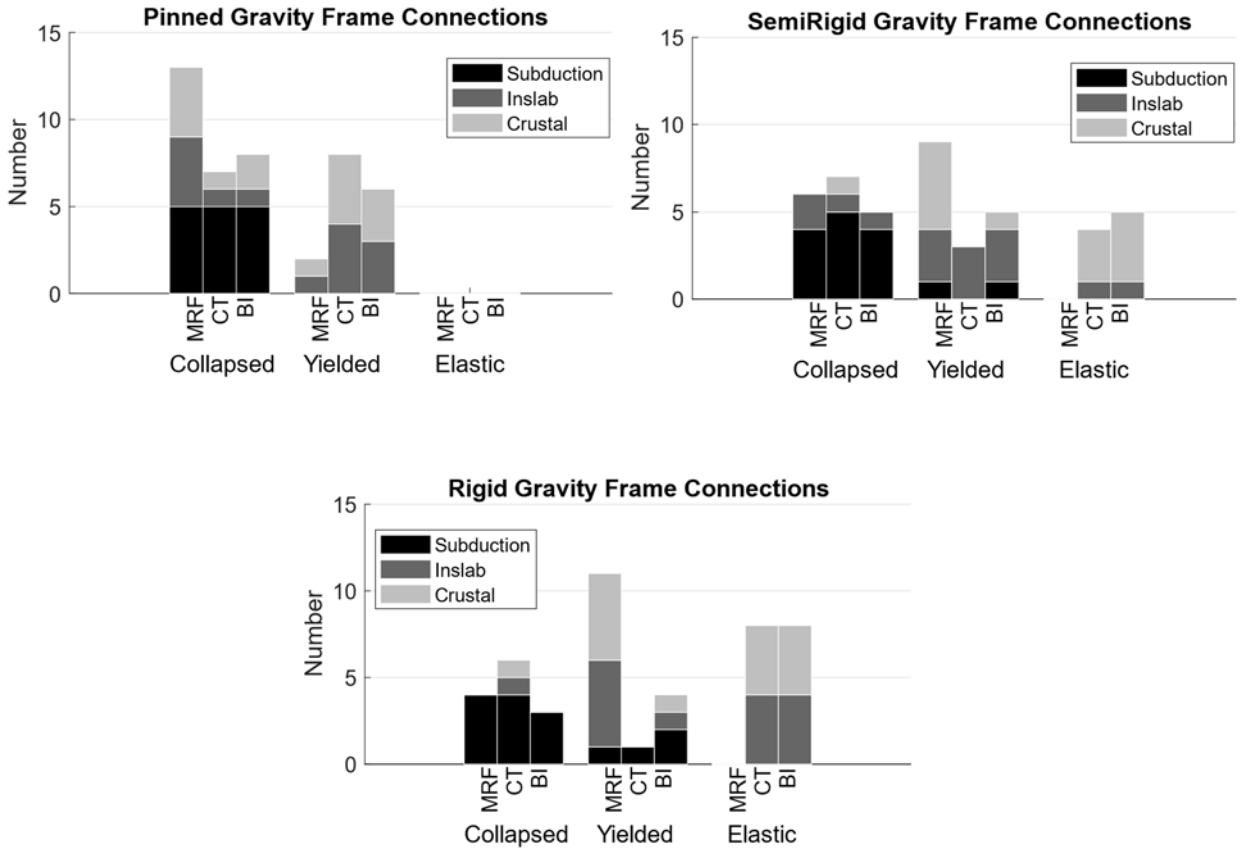

Figure 3: Number of ground motions causing collapse and yielding with different modeling assumptions under MCE crustal, inslab, and subduction ground motions

In comparison, the column-top (CT) isolated structure collapsed in 47% of the ground motions with pinned gravity connections but this number did not reduce with increasing rigidity of the gravity frame connections. Instead, the collapse mechanism of the column-top isolated structure shifted from excessive interstory drift in the superstructure to exceeding the bearing stability limit at large bearing displacements. As the superstructure became more rigid, the concentration of displacement at the isolation layer increased, decreasing the axial load carrying capacity of the bearings. The traditionally base isolated (BI) structure collapsed in 53% of the ground motions with pinned gravity connections but this reduced to 33% with semi-rigid connections. The collapse mechanism was generally initiated by excessive interstory drift as the base isolator had larger confining load, resulting in larger bearing designs and higher buckling capacity.

The peak interstory drifts are presented in Figure 4 for the pinned gravity frame, semi-rigid connection gravity frame, and rigid connection gravity frame. The line style (defined in legend) denotes the system evaluated while the line colour denotes the ground motion so that direct comparisons of interstory drift can be drawn on a motion by motion basis. The average reductions in drift and acceleration demand are presented in Table 5 and 6, respectively based on non-collapsed cases. Since the systems generally performed poorly during subduction earthquakes, there are few data points for those ground motions. Bolded values indicate larger reductions than the alternative isolation strategy. The average drift and acceleration reductions presented are a direct comparison of the story levels above the column-top isolation plane for both the base isolated and column-top structures. This is because the column-top structure is only isolated above the stiffened first floor columns. Modelling with the semi-rigid gravity connection assumption resulted in an average bearing displacement demand increase of 28% when compared to the pinned system and significantly decreased interstory drift demand. In many crustal and inslab ground motions, the superstructure stayed elastic or exhibited minor yielding when semi-rigid connections were considered. This is because the stiffness contribution of the semi-rigid connections resulted in better spaced isolated and fixed base first mode fundamental periods when compared to the pinned system. Introducing the shear tab connection stiffness contributions into the system will likely provide a more accurate estimate of isolator displacement demands but modelling the connections as pinned will provide a conservative estimate of superstructure drift demands. In retrofit scenarios for steel MRF structures, it is recommended to model and analyze the post-retrofit isolated structure in two separate cases: 1) Using pinned gravity frame connections to establish conservative drifts demands for the superstructure and 2) Using semi-rigid gravity frame connections to establish conservative drift demands for the isolators.

Table 5 Mean Interstory Drift Reductions in Percent (Excluding Collapsed Cases)

Ground Motion Type	Pinned		Semi-Rigid		Rigid	
	BI	CT	BI	CT	BI	CT
Crustal	20.3	**32.9**	35.0	**47.3**	44.4	**51.5**
Inslab	22.1	**26.8**	33.0	**42.0**	45.5	**57.4**
Subduction	-	-	**34.2**	-	**45.0**	18.1

Table 6 Mean Floor Acceleration Reductions in Percent (Excluding Collapsed Cases)

Ground Motion Type	Pinned		Semi-Rigid		Rigid	
	BI	CT	BI	CT	BI	CT
Crustal	**36.0**	32.2	**38.5**	37.8	47.5	**49.2**
Inslab	**40.55**	31.2	**37.5**	36.4	**45.3**	45.6
Subduction	-	-	**30.4**	-	**32.7**	25.1

The isolated systems provide significant reductions to interstory drift and acceleration demands under crustal and inslab earthquakes. The column-top isolation system results in higher interstory drift reduction than the base isolation system for low rise MRF structures. The base isolation system tends to provide greater reductions in floor acceleration. Based on a few non-collapsed cases, the base isolated structure tends to perform better than the column-top isolated building during the long period subduction ground motions.

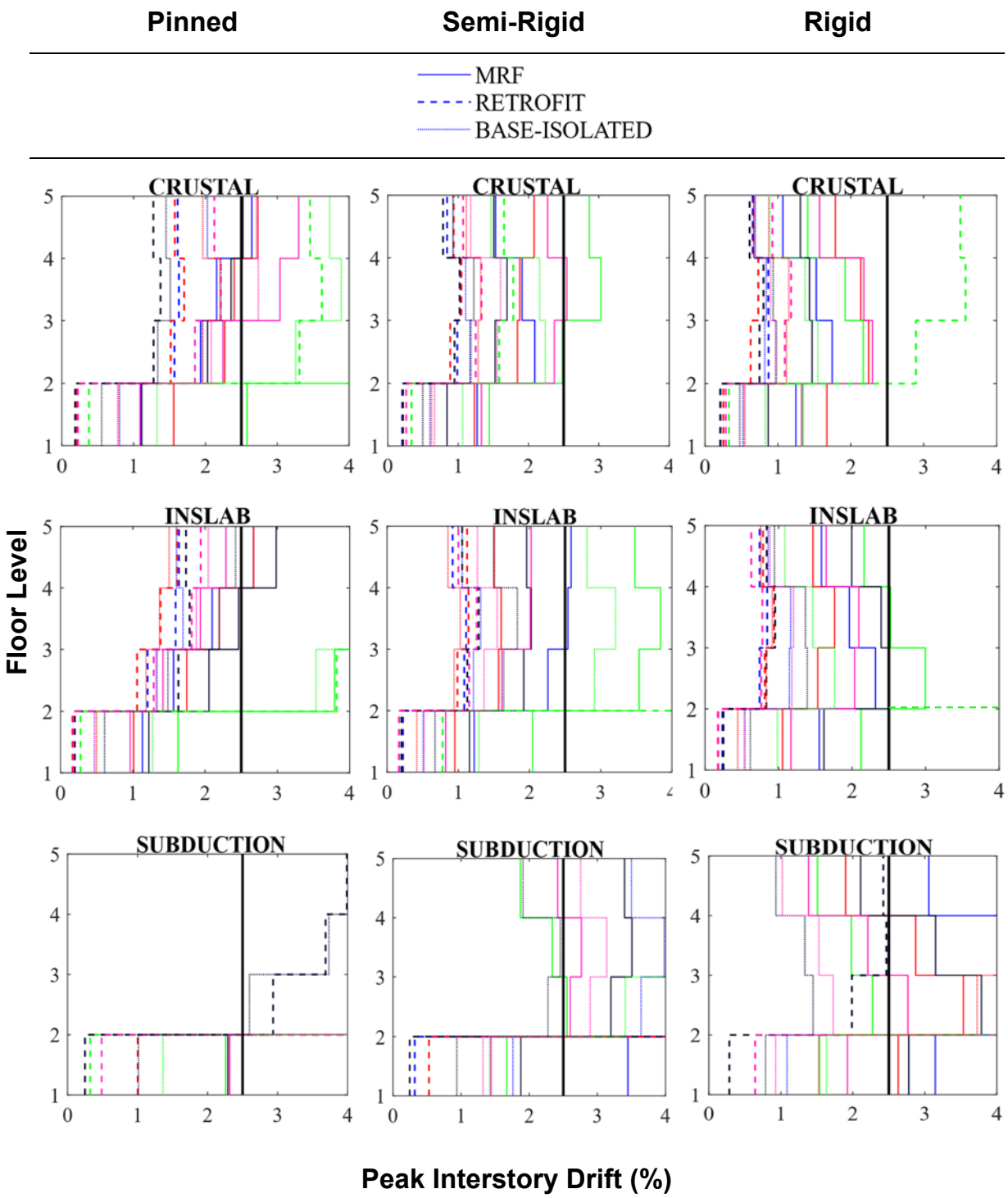

Figure 4: Peak Interstory Drifts for Pinned (Left), Semi-Rigid (Middle) and Rigid (Right) scenarios

4 CONCLUSIONS

The viability of a column-top lead-core rubber bearing isolation retrofit was numerically assessed for a steel pre-Northridge MRF office building located in Vancouver and compared to a traditional base isolation retrofit. The impacts of gravity frame connection fixity assumptions were assessed using pinned, semi-rigid, and rigid connections. It was found that achieving long, well-separated periods and sufficient damping is difficult for column-top isolation with rubber bearings due to light axial loads, resulting in bearing designs with smaller areas. The column-top isolation retrofit design generally resulted in lower interstory drifts and higher floor accelerations than the base isolation retrofit under crustal and inslab earthquakes based on non-collapsed cases; However, base isolation resulted in fewer collapses than column-top isolation with increasing superstructure rigidity. All systems performed poorly under subduction earthquakes due to their long fundamental periods. It is not recommended to use rubber bearing column-top isolation in a subduction zone because of the large displacement demand and lower buckling capacity of column-top isolation designs.

For column-top isolation, the pinned gravity frame modelling assumption resulted in ineffective displacement concentration at the isolation system and high superstructure demands. The higher superstructure demands led to the isolated structures yielding or collapsing in all ground motions as a result of excessive interstory drifts. The isolation retrofits performed significantly better when semi-rigid connections modelled as locally weakened fiber elements were introduced into the system. This resulted in an average 28% increase in bearing displacement and interstory drift reductions greater than 40% for crustal and inslab earthquakes. As a result, both pinned and semi-rigid gravity frame connection cases should be considered when modelling a column-top isolation system. This should be done to capture the potential for large interstory drift and excessive bearing displacement, providing conservative boundary demands for the superstructure in the pinned case and bearing demands in the semi-rigid case.

Recommendations for further work in this area include modeling system behaviour when lead-core rubber bearings are replaced with friction pendulum bearings to achieve longer isolation periods and suitable displacements capacity, evaluating the effectiveness of column-top isolation when used in stiffer building types, and using more refined models to more accurately represent the plastic behaviour of semi-rigid connections.

References

AISC. 2016. *ANSI/AISC 360-16: Specification for Structural Steel Buildings,* American Institute of Steel Construction, Chicago, IL, USA.

Barber, M.A., Rassati, G. A., Swanson, J. A. 2011. Contribution of shear connections to the lateral stiffness of steel frames. *Behaviour of Steel Structures in Seismic Areas*, 491-496.

CISC. 2014. *Handbook of Steel Construction, 11th ed*., Canadian Institute of Steel Construction, Markham, ON, Canada.

Crowder, A. P. and Becker, T. C. 2017. Experimental investigation of elastomeric isolation bearings with flexible supporting columns. *Journal of Structural Engineering*. ASCE, **143**(7).

CSA. 2014. *S16-14 Design of Steel Structures.* Canadian Standards Association, Mississauga, ON, Canada.

Goda, K. and Atkinson, G. M. 2011. Seismic performance of wood-frame houses in south-western British Columbia, *Earthquake Engineering and Structural Dynamics,* J Wiley, **40**: 903-924.

Hodgson, J. H. 1956. *A Seismic Portability Map for Canada.* National Research Council Canada, Ottawa, ON, Canada.

Imbimbo M. and Kelly, J. M. 1997. Stability aspects of elastomeric isolators, *Earthquake Spectra*, EERI, **13**(3): 431-449.

Jones, S. W., Kirby, P. A., and Nethercort, D. A. 1983. The analysis of frames with semi-rigid connections - A state-of-the-art report. *Journal of Constructional Steel Research*, Elsevier, **3**(2): 2-13.

Kumar, M., Whittaker, A., and Constantinou, M. 2015. Response of base-isolated nuclear structures to extreme earthquake shaking. *Nuclear Engineering and Design,* Elsevier, **295**(15): 860-874.

Kunnath S.K., Hoffmann G., and Reinhorn A.M. 1995. Gravity-load-designed reinforced concrete buildings-Part I: seismic evaluation of existing construction. *ACI Structural Journal*, ACI, **92**(3):343–354.

Lignos, D.G. and Krawinkler. H. 2012. Development and Utilization of Structural Component Databases for Performance Based Engineering. *Journal of Structural Engineering*, ASCE, **139**(8).

Liu, J and Astaneh-Asl, A. 2000. Cyclic Testing of Simple Connections Including Slab. *Journal of Structural Engineering.* ASCE. **126**(1): 32-39

McKenna, F. and Fenves, G. L. 2006. Open System for Earthquake Engineering Simulation (OpenSees), *Pacific Earthquake Engineering Research Center*, [Online].

NRCC. 1965. *National Building Code of Canada 1965*, National Research Council Canada, Ottawa, ON, Canada.

NRCC. 2015. *National Building Code of Canada 2015*, National Research Council Canada, Ottawa, ON, Canada.

Ramirez, C.M, Lignos, D.G, Miranda, E., and Kolios, D. 2012. Fragility functions for pre-Northridge welded steel moment-resisting beam-to-column connections. *Engineering Structures*, Elsevier, **45**: 574-584

Tremblay, R., Atkinson, G. M., Bouannani, N., Daneshvar, P., Léger, P. and Koboevic, S. 2015. Selection and scaling of ground motion time histories for seismic analysis using NBCC 2015, *11th Canadian Conference on Earthquake Engineering*, Victoria, BC, Canada.